# DISCRETE SYMMETRIC IMAGE REGISTRATION

*Aristeidis Sotiras* *Nikos Paragios*

Center for Visual Computing, Ecole Centrale Paris, Châtenay-Malabry, France
Equipe GALEN, INRIA Saclay - Ile-de-France, Orsay, France
Universite Paris-Est, LIGM (UMR CNRS), Center for Visual Computing, Ecole des Ponts ParisTech, FR

## ABSTRACT

Image registration is in principle a symmetric problem. Nonetheless, most intensity-based non-rigid algorithms are asymmetric. In this paper, we propose a novel symmetric deformable registration algorithm formulated in a Markov Random Fields framework where both images are let to deform towards a common domain that lies halfway between two image domains. A grid-based deformation model is employed and the latent variables correspond to the displacements of the grid-nodes towards both image domains. First-order interactions between the unknown variables model standard smoothness priors. Efficient linear programming is consider to recover the optimal solution. The discrete nature of our algorithm allows the handling of both mono- and multi-modal registration problems. Promising experimental results demonstrate the potentials of our approach.

***Index Terms*—** Symmetry, MRF, discrete optimization, deformable registration

## 1. INTRODUCTION

Deformable image registration defined as the establishment of dense correspondences between two images is an important tool in medical image analysis. One can cite a number of important applications of deformable registration: i) multi-modality fusion, where complementary information stemming from different imaging devices is fused to facilitate diagnosis and treatment planning; ii) longitudinal studies, where the evolution of a disease is studied; and iii) population modeling, where one studies the normal anatomical variability of a structure of interest.

Deformable image registration is in principle a symmetric problem. Nonetheless, most methods that aim to tackle it are asymmetric. That is, when swapping the order of the input images, the obtained transformation is not the inverse of the one obtained before the swap. Asymmetry in registration is not only unintuitive but also undesirable as it introduces bias in the process.

Asymmetry was first studied in the context of *inverse consistent* methods [1]. These methods penalize the difference between the inverse of the forward transformation and the backward one. The drawback of this framework is that is only asymptotically symmetric when the weight of the penalty is too great. Moreover, it is based upon the estimation of the inverse of a transformation that is not necessarily invertible.

Another way to endow registration with the symmetric property is by evaluating the objective function in both image domains [2, 3]. This strategy results in an increased computational burden. More efficient approaches are the ones that consider inverse-invariant objective functions to symmetrize the problem. Such a direction was first taken in [4] while more recently a more extensive analysis was given in [5]. These methods by letting only one image deform towards the other may suffer from asymmetry due to numerical implementation issues.

The last approach one may consider consists in warping both images simultaneously towards a common domain [6, 7]. When considering a different flow for each image, the dimensionality of the solution space for the previous methods is twice the one for standard asymmetric approaches. Trying to limit the number of parameters, a number of methods have considered only one flow for both images [8, 9, 10].

Previous works are based upon continuous optimization methods. As a consequence, they are not modular with respect to the objective criterion and depend greatly on the initial conditions. Towards overcoming these shortcomings, methods based on discrete optimization methods have been proposed [11].

In this work, we present a novel symmetric registration method that is formulated as a Markov Random Field (MRF) permitting the use of discrete optimization techniques. Our approach enjoys modularity with respect to objective function and efficiency. In the proposed approach, both images are deformed towards a common domain that is enforced to be at the same distance (in an Euclidean sense) from the image domains similar to [8, 10].

## 2. METHODS

Let us consider two images, a source image $S : \Omega_S \mapsto \mathbb{R}$ and a target one $T : \Omega_T \mapsto \mathbb{R}$, where $\Omega_S$ and $\Omega_T$ denote respectively the source and the target image domain. We aim at computing two deformation fields, one from the common domain to the source image domain $\mathcal{T}_{CS} : \Omega_C \mapsto \Omega_S$ and one from the common domain to the target image domain $\mathcal{T}_{CT} : \Omega_C \mapsto \Omega_T$. That way, the warping from source domain to the target one can be calculated as $\mathcal{T}_{ST} = \mathcal{T}_{CT} \circ \mathcal{T}_{CS}^{-1}$. This implies an assumption for reasonable displacements or else asymmetry may be introduced due to interpolation errors.

In order for the common domain to be equidistant from the two image domains, the transformations $\mathcal{T}_{CS}$ and $\mathcal{T}_{CT}$ should satisfy the following constraint:

$$\mathcal{T}_{CS} + \mathcal{T}_{CT} = 0 \text{ or } \mathcal{T}_{CS} = -\mathcal{T}_{CT}. \quad (1)$$

The previous equation implies that the number of parameters is equal to the one of standard asymmetric registration. Moreover, to allow the computation of the complete flow that maps from the one image to the other, the deformation should be invertible. In the proposed framework, the deformation is guaranteed to be diffeomorphic, that is one-to-one and smooth.

### 2.1. Deformation Model

We consider a grid-based deformation model that can satisfy the requirement for smooth and invertible transformations. The basic idea

of the deformation model consists in superimposing a grid $G$ onto the image to be deformed. The grid consists of $k$ control points distributed uniformly along the image domain ($k$ is smaller than the dimensionality of the domain). The embedded image can then be deformed by manipulating the grid control points.

The dense deformation field is given by assuming an interpolation strategy:

$$\mathcal{T}(\mathbf{x}) = \mathbf{x} + \sum_{i=1}^{k} \omega_i(\mathbf{x})\mathbf{d}_i, \tag{2}$$

where $\mathbf{d}_i$ denotes the displacement of the $i$th grid control point. In our context, the weight $\omega_i$ that determines the influence of the $i$th grid control point is determined assuming a cubic $B$-spline interpolation scheme. This choice is dictated by the existence of simple hard constraints on the control point displacements to guarantee the preservation of topology. Specifically, the maximum displacement should not exceed $0.4$ times the control point spacing [12].

Given that two transformations need to be estimated, two isomorphic deformation grids ($G_{CS}$ and $G_{CT}$) are employed. Taking into consideration the deformation model, the constraint in Eq. 1 can be expressed as:

$$\mathbf{d}_{i,CS} = -\mathbf{d}_{i,CT}. \tag{3}$$

As the previous equation suggests, one parameter has to be estimated for each node and depending on which deformation field is considered, its positive or negative value will be used.

### 2.2. Discrete Symmetric Registration

Mathematically, image registration is usually cast as an energy minimization problem. In a discrete setting, the problem is formulated with the use of MRF. In the specific context, the solution space is quantized and represented by a discrete set of plausible solutions or labels $\mathcal{L}$. The goal is to estimate the optimal label assignment by a minimizing an energy of the following form:

$$E_{MRF} = \sum_{p\in\mathcal{V}} \mathcal{U}_p\left(l_p\right) + \sum_{pq\in\mathcal{E}} \mathcal{P}_{pq}\left(l_p, l_q\right) \tag{4}$$

Typically, such a model is represented by a graph $\mathcal{G} = (\mathcal{V}, \mathcal{E})$, where $\mathcal{V}$ denotes the set of vertices while $\mathcal{E}$ the edge system. In this specific case, the graphical model has the same topology as the deformation grids. The set of nodes corresponds to control point displacements or a label assignment $l_p \in \mathcal{L}$ is equivalent to displacing the corresponding control point $p$ in both $G_{CS}$ and $G_{CT}$ by $\mathbf{d}^{l_p}$ and $-\mathbf{d}^{l_p}$ respectively $\left(l_p \equiv (l_{p,CS}, l_{p,CT}) \equiv \left(\mathbf{d}^{l_p}, -\mathbf{d}^{l_p}\right)\right)$. The neighborhood system follows a 6-connectivity scheme and models the interaction between variables that correspond to neighboring deformation nodes.

The explicit control that we have over the creation of the label set $\mathcal{L}$ enables us to impose explicitly desirable properties on the obtained solution. That is, by sampling the solution space so that Eq. 1 is satisfied $\left(l_p \equiv \left(\mathbf{d}^{l_p}, -\mathbf{d}^{l_p}\right)\right)$, the common domain is constrained to lie halfway between the two image domains. Moreover, by bounding the maximum displacement that is sampled by $0.4$ times the grid spacing, the resulting deformation is guaranteed to be diffeomorphic.

The MRF energy (Eq. 4) is given as a summation of unary potentials $\mathcal{U}$ and pairwise potentials $\mathcal{P}$. The unary potentials are used to model the data matching term while the pairwise potentials the smoothness term that is necessary to account for the ill-posedness of the registration problem as well as to introduce our prior knowledge regarding the solution. Let us now define them.

The unary potentials are defined as:

$$\mathcal{U}_p(l_p) = \int_{\Omega_C} \hat{\omega}_p(\mathbf{x})\, \rho(S \circ \mathcal{T}_{CS,l_{p,CS}}(\mathbf{x}), T \circ \mathcal{T}_{CT,l_{p,CT}}(\mathbf{x}))\, d\mathbf{x}, \tag{5}$$

where $\mathcal{T}_{CS,l_{p,CS}}$ denotes the transformation when a control point $p \in G_{CS}$ has been displaced by $l_{p,CS}$. $\mathcal{T}_{CT,l_{p,CT}}$ is defined similarly. $\rho$ denotes any intensity-based dissimilarity criterion while $\hat{\omega}_i$ is a weighting function similar to the one in Eq. 2. It determines the influence or contribution of an image point $x$ onto the (local) matching term of individual control points. Only image points in the vicinity of a control point are considered for the evaluation of the dissimilarity measure with respect to the displacement of this particular control point. This is in line with the local support that a control point has on the deformation.

The previous is valid when point-wise similarity criteria are considered. When an information theoretic criterion is to be used, a different definition of $\hat{\omega}_i$ is adopted,

$$\hat{\omega}_i(\mathbf{x}) = \begin{cases} 1, & \text{if } \omega_i(\mathbf{x}) \geq 0, \\ 0 & \text{otherwise.} \end{cases} \tag{6}$$

Thus, in both cases the criterion is evaluated on a patch. The only difference is that the patch is weighted in the first case. These local evaluations enhance the robustness of the algorithm to local intensity changes. Moreover, they allow for computationally efficient schemes.

The random variables are assumed to be conditionally independent. As a consequence, the unary potentials that constitute the matching term can only be an approximation to the real matching energy as the image deformation and thus the local similarity measure depends on more than one control point since their influence areas do overlap. Still, the above approximation yields very accurate registration. Furthermore, it allows an extremely efficient approximation scheme which can be easily adapted for parallel architectures yielding extremely fast cost evaluations

The unary potentials can be seen as encoding an overlapping blocks matching strategy. The evaluation of the unary potentials for a label $l \in \mathcal{L}$ corresponding to the displacements $\mathbf{d}_{CS}$ and $\mathbf{d}_{CT}$ can be efficiently performed as follows. First, each image is globally translated by applying the respective displacement. In the overlapping domain, the unary potentials for this label and for all control points are calculated simultaneously. This result in a one pass through the common domain to calculate the cost and distribute the local energies to the graph nodes. The constrained transformation in the unary potentials is then simply defined as $\mathcal{T}_{\text{ico},CS,l_{p,CS}}(\mathbf{x}) = \mathcal{T}_{\text{ico},CS}(\mathbf{x}) + l_{p,CS}$, where $\mathcal{T}_{\text{ico},CS}(\mathbf{x})$ is the current or initial estimate of the transformation. From a computational point of view, the extra load w.r.t the asymmetric registration is minimal and stems from the fact that both images are transformed simultaneously. As a result, the number of interpolation operations that are performed is doubled. An insignificant cost to pay to symmetrize the registration process.

The pairwise potentials penalize deviations of displacements of neighboring control points in both deformation grids. The basic assumption is that control points that are close should behave in a similar way. Two different types of pairwise potentials may be defined depending on the nature of the smoothness constraint we want to model. Due to the nature of the displacements consider here, the

pairwise potentials are defined considering only the transformation from the common domain to the source one.

If we consider an elastic-like regularization, an efficient discrete approximation can be defined as

$$\mathcal{P}_{\text{elastic},CS,pq}(l_p, l_q) = \frac{\|(\mathbf{d}_{p,CS} + l_{p,CS}) - (\mathbf{d}_{q,CS} + l_{q,CS})\|}{\|\mathbf{p} - \mathbf{q}\|}, \tag{7}$$

where $\mathbf{d}_p$ and $\mathbf{d}_q$ denote the current displacements of the control points $p$ and $q$. If we remove the current displacements from the previous definition, the fluid-like behavior can be obtained that penalizes only the difference between the incremental displacement of the deformation field:

$$\mathcal{P}_{\text{fluid},CS,pq}(l_p, l_q) = \frac{\|l_{p,CS} - l_{q,CS}\|}{\|\mathbf{p} - \mathbf{q}\|}. \tag{8}$$

In the fluid-like behavior case, all edges share the same pairwise potential function resulting in low memory and computational demands.

## 3. EXPERIMENTAL VALIDATION

To validate the performance of the proposed framework a 3D brain MRI data set was used. The data set consists of 18 T1-weighted brain volumes that have been positionally normalized into the Talairach orientation (rotation only). The MR brain data set along with manual segmentations was provided by the Center for Morphometric Analysis at Massachusetts General Hospital and are available online[1]. The data set was rescaled and resampled so that all images have a size equal to $256 \times 256 \times 128$ and a physical resolution of approximately $0.9375 \times 0.9375 \times 1.5000$mm.

Our validation setting is constructed upon the comparison of the proposed framework with the one proposed in [7]. The reason behind our choice is threefold. First, the symmetric diffeomorphic registration framework is considered state-of-the-art and has demonstrated extensively its effectiveness in MRI Brain registration [13]. Second, the source code is publicly available[2] allowing for a straightforward comparison. Third, it is based on a similar strategy to symmetrize the registration problem. Despite the fact that [7] has significantly more degrees of freedom, useful conclusions may be drawn by the comparison of the two methods.

In our experiments, we used a multiresolution scheme in order to harness the computational burden. A three-level image pyramid was considered while a deformation grid of four different resolutions was employed. The two finest grid resolutions operated on the finest image resolution. The two coarsest operated on the respective coarse image representations. The initial grid spacing was set to 40mm resulting in a deformation grid of size $7 \times 7 \times 6$. The size of the gird was doubled at each finer resolution. A number of 90 labels, 30 along each principal axis, were used. The maximum displacement indexed by a label was bounded to 0.4 times the grid spacing. Normalized Cross Correlation was used as data cost while the fluid-like regularization (Eq. 8) was preferred due to its low computational and memory demands. The pairwise potentials were weighted by a factor of 0.1. An efficient linear programming technique [14] was employed to optimize the resulting energy.

Regarding [7], we used as similar parameters to ones used in the evaluation study [13] as possible. The following command was used to obtain the reported results:

```
ANTS 3 -m CC[<target>.nii, <source>.nii, 1, 5]
 -o <output transform>.nii -r Gauss[2,0]
 -t SyN[0.5] -i 30x99x11
 -number-of-affine-iterations 1x1x1
```

Instead of using the probabilistic metric, the advised Cross Correlation was used as it also facilitates the comparison between the two methods. The minimum number of iterations for the available affine registration step was used for fairness reasons.

To evaluate the performance of the algorithms, an image was selected randomly as a template and all the rest were registered to it. In order to assess visually the performance of both methods, the mean intensity image of the deformed images on the target domain was calculated and is depicted in the first row of Fig. 1. Both methods produce sharp mean images that is a clear indication of good performance. In the second row of Fig. 1 the used target image is shown as well as a deformed image produced with each method. While our proposed method has produced a good result, the one given by [7] has recovered more details.

Furthermore, a quantitative analysis was performed based on the manual segmentations of the gray (GM) and white matter (WM) that are available in the data set. In Fig. 2 we report the boxplots of the DICE criterion for the WM and GM classes. For the sake of comparison, the values before registration are also provided. When comparing with the baseline, one may conclude that both methods have performed well. The high DICE values are an indication of good performance. Clearly, [7] has performed slightly better than the proposed method.

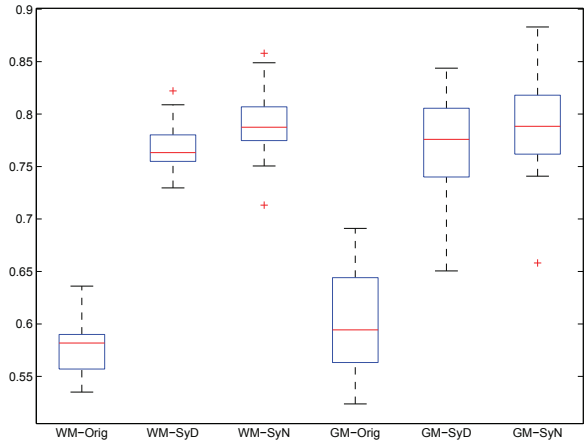



**Fig. 2:** Boxplots for the DICE criterion initially, with our method and with [7]. On the left, the results for the WM. On the right, the results for the GM.

To conclude this section, let us point out that the results reported for our method were obtained in 10 min. On the contrary, in order to obtain the results with [7] approximately 1 hour was necessary. We firmly believe that the important difference in the computational efficiency between the two methods can outweigh the slight difference in the quality of the solution in practice.

## 4. DISCUSSION

In this paper, we introduced a novel method for symmetric image registration. The main contribution of the proposed approach lies

[1] http://www.cma.mgh.harvard.edu/ibsr/data.html
[2] http://picsl.upenn.edu/ANTS/

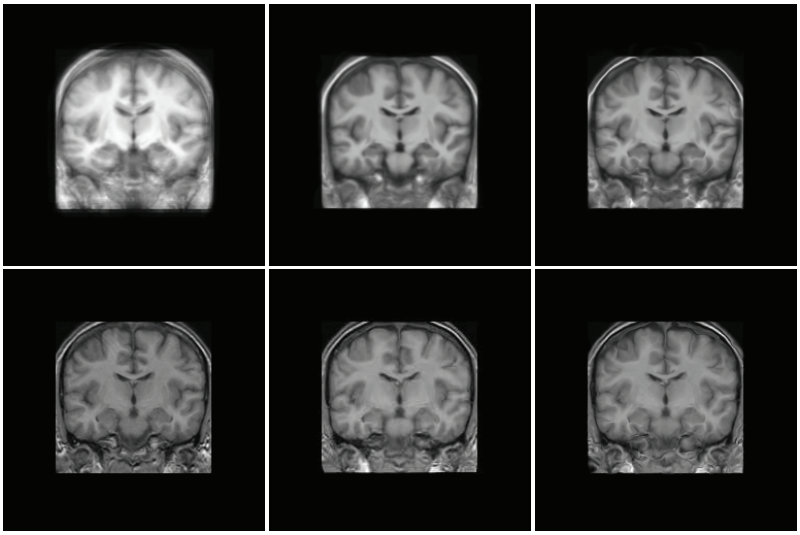


**Fig. 1:** In the first row, from left to right, the mean intensity image is depicted for the data set, after the proposed method and after [7]. In the second row, from left to right, the target image is shown as well as a typical deformed image for the proposed method and [7]. For all cases, the central slice is depicted.

in the Markov Random Field formulation of the problem. The control over the candidate solutions enabled us to introduce desirable constraints on the obtained deformation fields. A major trait of the proposed scheme is its extreme efficiency that is derived from both the efficient linear programming optimization and our cost evaluation strategy. We should underline that the registration framework was endowed with the symmetric property at minimal extra computational cost. Last not least, we should note that our method is highly parallelizable and thus a GPU implementation could further improve its computational performance.

## 5. REFERENCES


[1] Gary E. Christensen and Hans J. Johnson, "Consistent image registration.," *IEEE TMI*, vol. 20, no. 7, pp. 568–82, jul 2001.

[2] Alex D. Leow, Sung-Cheng Huang, Alex Geng, James Becker, Simon Davis, Arthur W. Toga, and Paul M. Thompson, "Inverse consistent mapping in 3D deformable image registration: its construction and statistical properties.," in *IPMI*, jan 2005, vol. 19, pp. 493–503.

[3] Tom Vercauteren, Xavier Pennec, Aymeric Perchant, and Nicholas Ayache, "Symmetric log-domain diffeomorphic Registration: a demons-based approach.," in *MICCAI*, jan 2008, pp. 754–61.

[4] Pascal Cachier and David Rey, "Symmetrization of the non-rigid registration problem using inversion-invariant energies: application to multiple sclerosis," in *MICCAI*, 2000, pp. 697–708.

[5] Hemant Tagare, David Groisser, and Oskar Skrinjar, "Symmetric non-rigid registration: A geometric theory and some numerical techniques," *JMIV*, vol. 34, no. 1, pp. 61–88, 2009.

[6] Sarang C. Joshi, Brad Davis, Matthieu Jomier, and Guido Gerig, "Unbiased diffeomorphic atlas construction for computational anatomy.," *NeuroImage*, pp. S151–60, jan 2004.

[7] Brian B. Avants, C L Epstein, M Grossman, and James C. Gee, "Symmetric diffeomorphic image registration with cross-correlation: evaluating automated labeling of elderly and neurodegenerative brain.," *MedIA*, pp. 26–41, 2008.

[8] Vincent Noblet, Christian Heinrich, Fabrice Heitz, and Jean-Paul Armspach, "Symmetric nonrigid image registration: application to average brain templates construction.," in *MICCAI*, jan 2008, vol. 11, pp. 897–904.

[9] Mirza Faisal Beg and Ali Khan, "Symmetric data attachment terms for large deformation image registration.," *IEEE TMI*, vol. 26, no. 9, pp. 1179–89, sep 2007.

[10] Colin Studholme, Corina Drapaca, Bistra Iordanova, and Valerie Cardenas, "Deformation-based mapping of volume change from serial brain MRI in the presence of local tissue contrast change.," *IEEE TMI*, pp. 626–39, 2006.

[11] Ben Glocker, Aristeidis Sotiras, Nikos Komodakis, and Nikos Paragios, "Deformable medical image registration: setting the state of the art with discrete methods.," *AR*, vol. 13, pp. 219–44, aug 2011.

[12] Daniel Rueckert, Paul Aljabar, Rolf A. Heckemann, Joseph V. Hajnal, and Alexander Hammers, "Diffeomorphic registration using B-splines.," in *MICCAI*, jan 2006, vol. 9, pp. 702–9.

[13] Arno Klein, Jesper Andersson, Babak A. Ardekani, John Ashburner, Brian B. Avants, Ming-Chang Chiang, Gary E. Christensen, D. Louis Collins, James C. Gee, Pierre Hellier, Joo Hyun Song, Mark Jenkinson, Claude Lepage, Daniel Rueckert, Paul M. Thompson, Tom Vercauteren, Roger P Woods, J John Mann, and Ramin V Parsey, "Evaluation of 14 nonlinear deformation algorithms applied to human brain MRI registration.," *NeuroImage*, pp. 786–802, 2009.

[14] Nikos Komodakis, Georgios Tziritas, and Nikos Paragios, "Performance vs computational efficiency for optimizing single and dynamic MRFs: Setting the state of the art with primal-dual strategies," *CVIU*, vol. 112, no. 1, pp. 14–29, oct 2008.